# Principle Of A Hybrid Compressed Air And Supercapacitors Energy Storage System With Maximum Efficiency Point Tracking

S. Lemofouet,[1] A. Rufer, P. Barrade, F. Grasser, Swiss Federal Institute of Technology, Lausanne, Switzerland

**Abstract**

This paper presents a hybrid energy storage system based on Compressed Air Energy Storage (CAES), where the extraction of energy is done within maximum efficiency conditions. As the maximum efficiency conditions impose the level of converted power, an intermittent time-modulated operation mode is applied to the thermodynamic converter to obtain a variable converted power. A smoothly variable output power is achieved with the help of a supercapacitive auxiliary storage device. The paper describes the concept of the system, the power-electronic interface circuits and especially the Maximum Efficiency Tracking algorithm and the strategy used to vary the output power. Practical results are also presented, recorded from a low-power pneumatic motor coupled to a small DC generator.

**Introduction**

World wide, considerations have been made on energy resources, about traditional generation and distribution systems as well as renewable means. Traditionally, energy storage has been of high interest, as in the case of not flexible nuclear or thermal power versus daily cycles [1], [2]. In the context of energy storage in relation with power generation, the issues of fast and strong load variations have also been studied [3], [4]. For the future concepts of energy production and distribution, like decentralized generation, balancing of production and consumption is one of the main concerns. Because of the loss of the effect of a "statistical mean value" of loads, that normally smoothes their profile, the principle of decentralized generation could present some risks both for generators and loads, which will reinforce the need of storage facilities. Concerning the integration of renewable means, like photovoltaic and wind power, that are intermittent sources, additional storage means are also required.

Recently several new storage technologies have appeared, as alternative solutions to classical batteries, and are integrated in real networks [5], [6]. CAES technologies belong to these innovative developments, with their high potential of producing less problematic waste materials. In fact, they have been proposed from longer date, in the middle and high power range, as well as in transportation and generation of electrical power. Ultra-large size facilities have been proposed recently based on dedicated turbo machinery [7]. Several small size accumulators have also been proposed using intermediary mechanical/hydraulic conversion with the so-called "liquid piston" principle. [13]

In the present study, a low cost vane type pneumatic motor has served as example of a thermodynamic expansion converter, with the goal of developing operation and control strategies in order to avoid the use of dissipating valves between the air tank and the converter and optimize the energy conversion. A supercapacitive auxiliary storage device is used to smooth the intermittent resulting power. The concept of the hybrid CASCES (Compressed Air and Supercapacitors Energy Storage) system is described first, then the Maximum Efficiency Point Tracking algorithm is presented and finally, the strategy for varying the electric output power is proposed.

**1- Principle of hybrid CASCES System**

The idea of associating a high capacity energy storage medium (compressed air), and a high power density storage device (supercapacitors), is implemented in the context of an off-line UPS system whose principle is presented in figure 1. All the devices of the system are reversible. During the storage process, the electric machine works as a motor and drives the pneumatic machine, which operates as a compressor to fill the vessel with high-pressure air. During the generation process, the compressed air is directly expanded in the pneumatic machine, which operates as motor to power the DC generator. The following technical solutions have been implemented to improve the reliability and efficiency of the system:

- There is no pressure regulation device between the air tank and the pneumatic machine in order to avoid the important losses in such a device. The motor inlet pressure therefore varies continuously.

[1] sylvain.lemofouet@epfl.ch

- An efficiency optimization algorithm has been developed to control the pneumatic machine through variable speed, so as to always keep it at the maximum efficiency operating point. This aims at reducing energy consumption during compression and to maximizing the efficiency during generation.

- Since the maximum efficiency operation is conditioning the produced power level, an intermittent operation mode is used to modulate the produced power as a function of the output power demand.

- The supercapacitive auxiliary storage device is therefore necessary to obtain a smoothly variable high quality output power, through the regulation of the capacitive intermediary stage voltage.

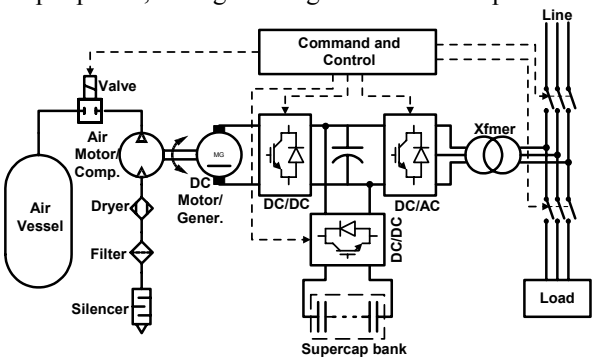


**Figure 1: Principle of CASCES system**

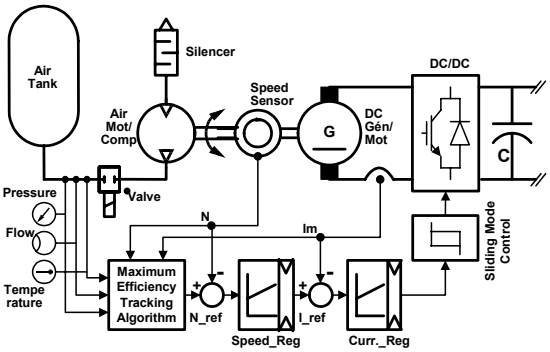


**Figure 2: Principle of Efficiency optimization**

## 2- Strategy of Efficiency Optimization

### 2.1- Principle of Efficiency optimization

The continuous changes in pressure and load affect the pneumatic machine's performances, namely the efficiency. The purpose of the efficiency optimization strategy is to control the operating point so as to optimize the energy conversion. The principle of this strategy is given in figure 2. On the basis of various measurements (pressure, flow rate, speed, etc), the maximum efficiency-tracking module determines the optimal speed, which corresponds to the maximum efficiency. This optimal speed serves as reference to the speed control module and is achieved by acting on the electromagnetic torque of the DC generator trough the current by means of the current regulator and the DC-DC converter as shown in figure 2. In order to study the Maximum Efficiency Point Tracking algorithm, a model of the pneumatic machine has to be built.

### 2.2- Model of pneumatic motor

The pneumatic actuator used in this study is a vane type air motor. It has the advantages of high speed, good compliance and high power-to-weigh and power-to-size ratios. Its main drawback is the low efficiency due to important internal friction and leakage [14]. But its characteristics are typical of volumetric machines and can be used to design a general algorithm for this type of machines. A representative model is built on the basis of the characteristic curves provided by the manufacturer. At the constant nominal pressure of 6.3bar, the mechanical torque $M_m$ and mechanical power $P_m$ can be given by:

$$M_m = M_o(1-\frac{N}{N_o}) \qquad (1) \qquad P_m = \frac{2\pi}{60} N.M_m = \frac{\pi}{30} M_o(N-\frac{N^2}{N_o}) \qquad (2)$$

where $M_o$ is the starting torque, $N$ the rotation speed and $N_o$ the free speed. The volumetric exhaust airflow rate $\dot{V}_o$ can be roughly estimated with the following equation:

$$\dot{V}_o = 10^{(c_1 N^2 + c_2 N + c_3)} \qquad (3)$$

where $c_1$, $c_2$, $c_3$ are interpolation constants.

The characteristics at variable pressure are obtained by including in the previous equations some correction functions. These functions describe the effect of pressure variation on the characteristics at constant nominal pressure. These functions are respectively for mechanical torque, free speed and airflow:

$$f_t = c_{t1} p + c_{t2} \qquad (4) \qquad f_n = c_{n1} p^2 + c_{n2} p + c_{n3} \qquad (5) \qquad f_a = c_{a1} p + c_{a2} \qquad (6)$$

where, $p$ is the pressure and $c_{t1}$, $c_{t2}$, $c_{n1}$, $c_{n2}$, $c_{n3}$, $c_{a1}$, and $c_{a2}$ are interpolation constants. The resulting equations for the characteristics at variable pressure are:

$$M_m = f_t.M_o(1-\frac{N}{f_n.N_o}) \quad (7) \qquad P_m = \frac{\pi}{30}N.M_m = \frac{\pi}{30}f_t.M_o(N-\frac{N^2}{f_n.N_o}) \quad (8)$$

$$\dot{V}_o = f_a.10^{(c_1N^2+c_2N+c_3)} \quad (9)$$

Figure 3 represents these characteristics for different values of pressure.

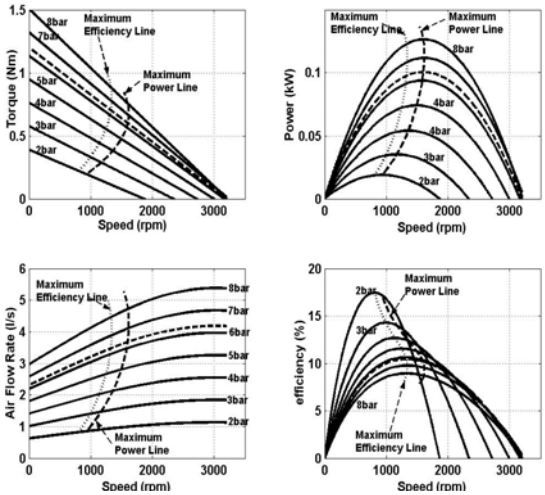


**Figure 3: Characteristics of air motor**

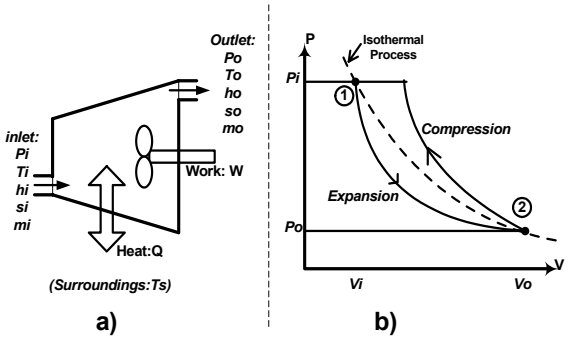


**Figure 4: Thermodynamic representation and P-V diagram of air motor**

### 2.3- Expression of Efficiency

In order to express the efficiency of the conversion, the air motor is modeled as an open thermodynamic system as shown in figure 4. Air is assumed to be a perfect gas with constant specific heats; the flow is considered as continuous and steady, and changes in kinetic and potential energies are negligible. In these conditions and according to the first and second laws of thermodynamic, the elementary work $dw$ of a unit mass of the flowing air is:

$dw \le dh - ds$ (10) where $dh$ and $ds$ are respectively the changes in enthalpy and entropy. By integrating the above equation from state 1 at the inlet to state 2 at the outlet using thermodynamic relation and considering that the air in the tank (inlet) is at ambient temperature ($T_s = T_i$), the maximum available work in a unit mass of air is: [11]

$$w = RT_i\left[\ln\frac{p_i}{p_o} + \frac{\gamma}{\gamma-1}\left(1-\frac{T_o}{T_i}-\ln\frac{T_i}{T_o}\right)\right] \quad (11)$$

where $p_i$ and $p_o$ are respectively the inlet and outlet pressures, $T_i$ and $T_o$ the inlet and outlet temperatures, $R$ the gas constant and $\gamma = c_p/c_v$ the ratio of specific heats. The theoretical available power $P_a$ in the air mass flow rate $\dot{m} = dm/dt$ is then:

$$P_a = \dot{m}\,w = \dot{m}\,RT_i\left[\ln\frac{p_i}{p_o} + \frac{\gamma}{\gamma-1}\left(1-\frac{T_o}{T_i}-\ln\frac{T_i}{T_o}\right)\right] \quad (12).$$

Using the following ideal gas relations:

$\dot{m} = \rho\dot{V} = \frac{p_i}{RT_i}\dot{V}_i = \frac{p_o}{RT_o}\dot{V}_o$ and $\frac{T_i}{T_o} = \left(\frac{p_i}{p_o}\right)^{\frac{\gamma-1}{\gamma}}$, equation (12) becomes:

$$P_a = \frac{\gamma}{\gamma-1}\left[\left(\frac{p_i}{p_o}\right)^{\frac{\gamma-1}{\gamma}} - 1\right]p_o\dot{V}_o \quad (13)$$

The isentropic energy efficiency $\eta$ is then:

$$\eta = \frac{P_m}{P_a} = \frac{\frac{\pi}{30} f_t . M_o (N - \frac{N^2}{f_n . N_o})}{\frac{\gamma}{\gamma - 1}\left[\left(\frac{p_i}{p_o}\right)^{\frac{\gamma-1}{\gamma}} - 1\right] p_o \dot{V}_o} \qquad (14)$$

Figure 3 represents the efficiency for different pressures and shows the maximum efficiency operating point.

**2.4- Maximum Efficiency Point Tracking (MEPT) algorithm.**

The expression of equation (14) is used as objective function for the efficiency optimization strategy. The shaded surface of figure 5 shows the variation of this function with respect to pressure *p* and speed *N*. The objective of the MEPT algorithm is to keep the working point of the air motor always at the top of this surface (bolt line). This is achieved with the combination of two techniques: Quadratic Interpolation and the so-called "Perturbation-Observation" technique.

- ***Quadratic Interpolation*** is used at start up to come rapidly and accurately close to the optimum. It's based on the quadratic shape of the efficiency as shown in Figure 5, which can be approximated as a second order polynomial function of speed. The optimal speed $N_{ref}$ that corresponds to maximum efficiency can be easily determined from three points (0;0), $(N_{k-1};t_{k-1})$ and $(N_k;t_k)$ which represent respectively the speed and efficiency at initial instant $t_0$, previous instant $t_{k-1}$ and present instant $t_k$, by:

$$N_{ref} = N_i = \frac{\eta_{k-1} N_k^2 - \eta_k N_{k-1}^2}{2(\eta_{k-1} N_k - \eta_k N_{k-1})} \qquad (15)$$

- Once the interpolated optimum is reached, it's tracked using the " ***Perturbation – Observation***" technique, [9] which consists of periodically incrementing or decrementing the speed and analyzing the resulting change in efficiency. The subsequent change in speed is performed so as to always move in the direction of rising efficiency. The flow diagram of figure 6 summarizes this MEPT algorithm. $N_{\lim}$ is the minimum difference between $N_k$ and $N_{k-1}$ that ensures the convergence of the quadratic interpolation. $\Delta N$ is the speed increment. It should be chosen judiciously to avoid instability of the algorithm and important mechanical constraints. In this case, a smooth and sensitive variation was performed with $3 \le \Delta N \le 5 rpm$

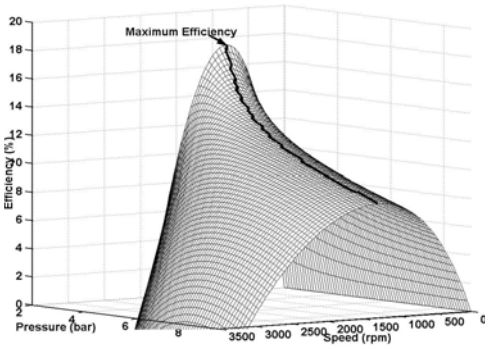


**Figure 5: Efficiency surface**

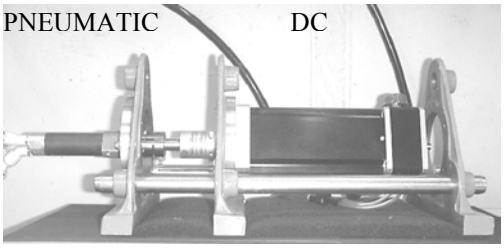


**Figure 7: Experimental bench**

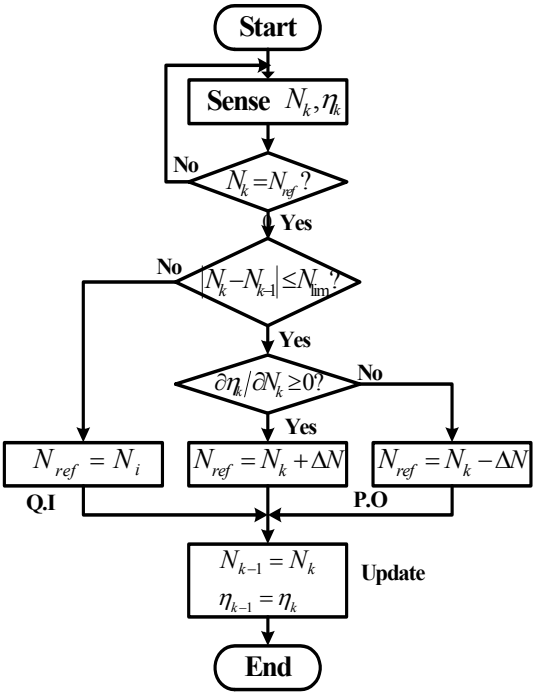


**Figure 6: Flow diagram of MEPT algorithm**

**2.5- Experimental Results**

The developed MEPT strategy has been applied on the 0.1kW air motor that is presented in Figure 7. The control algorithm was implemented on a DSP Board and performed with a sampling time of 0.2ms. The recorded responses are presented in Figure 8.

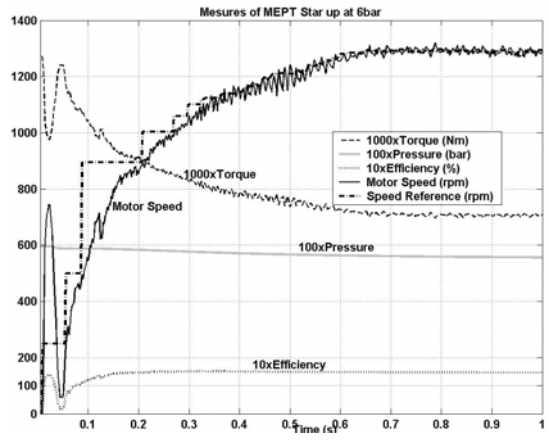


**Figure 8a: Experimental start up at 6bar**

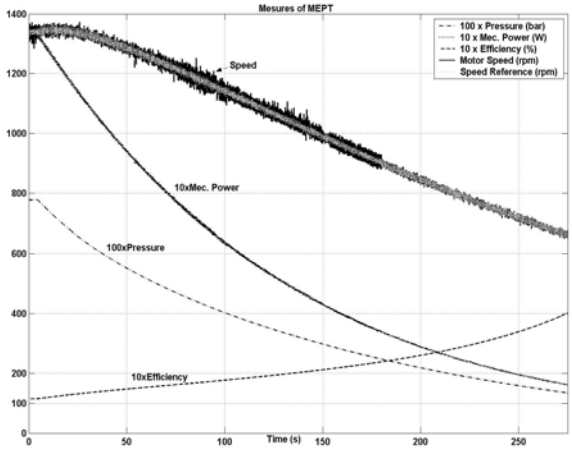


**Figure 8b: Experimental MEPT from 8bar**

As it can be seen on the start-up response of figure 8a, the system accurately reaches the optimal speed about 0.7s after the opening of the air valve. This delay is variable because of the random starting torque of vane type air motor. The tracking curves of figure 8b show a speed excursion of 20rpm around the mean value, mainly for high pressure. This is due to the nature of "Perturbation–Observation" technique used. But this excursion is small enough to ensure a smooth average speed. The performance of the presented METP algorithm can be appreciated on Figure 9, where the experimental optimum is represented versus the analytic optimum obtained by derivation of expression (14). The two curves are almost superposed, which shows the effectiveness and accuracy of the proposed algorithm. In addition, no particular knowledge of the air motor; therefore, it can be used efficiently to control of any type of volumetric machine.

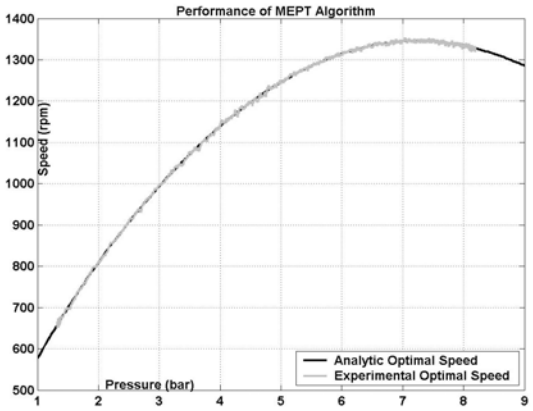


**Figure 9: Performance of MEPT Algorithm**

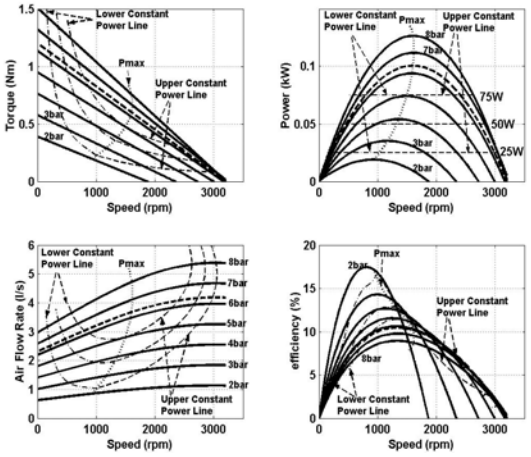


**Figure 10: Maximum and Constant power operating points**

### 3- Extension to Power-Tracking operation modes

The efficiency optimization strategy just presented can be easily extended to control the air motor in two power tracking modes, namely the **Maximum Power Point Tracking (MPPT)** operation mode and the **Random Power Point Tracking (RPPT)** operation mode. It's important to note that these power-tracking modes are done at the expense of conversion efficiency. The RPPT mode can be used for example in applications without an auxiliary storage device, to balance the generated power with the load power. The MPPT can be used in the case of temporary peak power demand.

### 3.1- Maximum Power Point Tracking (MPPT) Operation Mode

The expression of the objective function in this mode is given in equation (8). Figures 3 and 10 show the maximum power operating line for different pneumatic motor's characteristics. As it can be seen, the speed of

the maximum power point is higher than that of the maximum efficiency point. The MPPT operation is achieved with the same base algorithm of figure 6, by replacing the efficiency $\eta$ with the power $P_m$. Experimental results have also confirmed the effectiveness of the algorithm in this case.

### 3.2- Random Power Point Tracking (RPPT) Operation Mode

The RPPT operation mode consists of driving the pneumatic machine so as to generate any power reference. Figure 10 shows that for a given power, two operating points are possible, on both sides of the maximum power point. But the one off lower speed has a better efficiency and is considered as target optimum in this operation mode. The RPPT operation is achieved with the algorithm described by the flow diagram of figure 11. The tracking method is mainly the "Perturbation-Observation" technique presented earlier. As the pressure drops during generation, it's not always possible to deliver the desired power. When the minimum pressure for a given power is reached, the system can either stop as shown in the flow diagram or switch to the MPPT mode as shown on the experimental results of figure 12.

## 4- Strategy of output power variation

### 4.1- Principle

As mentioned earlier, the variation of electric output power $P_L$ is based on intermittent, time-modulated operation of the thermodynamic conversion. The excess of resulting intermittent power $P_e$ is stored in the supercapacitive device and used to supply the load during the stop-time of the pneumatic machine or as power assistance during peak power demand. The control scheme of this strategy is presented in figure 13. By maintaining the intermediary voltage $U_{\_\text{inter}}$ constant, the voltage regulator automatically compensates the lack or excess of converted power, allowing thus the output power to vary freely. The PWM on-off operation of the thermodynamic conversion is done through the electro valve control module. There are two possible operation modes: fixed frequency operation mode and free oscillating operation mode.

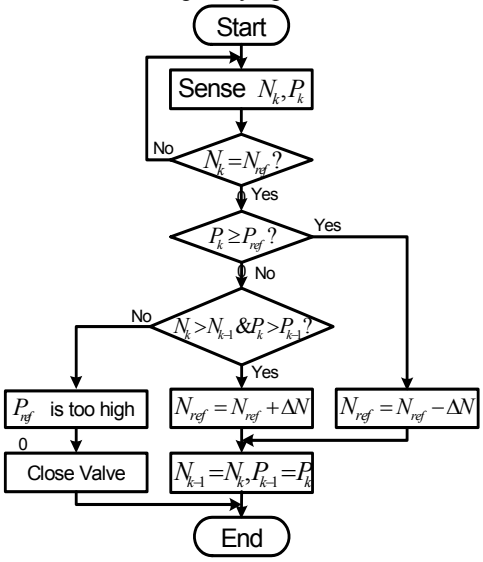


**Figure 11: Flow diagram of RPPT algorithm**

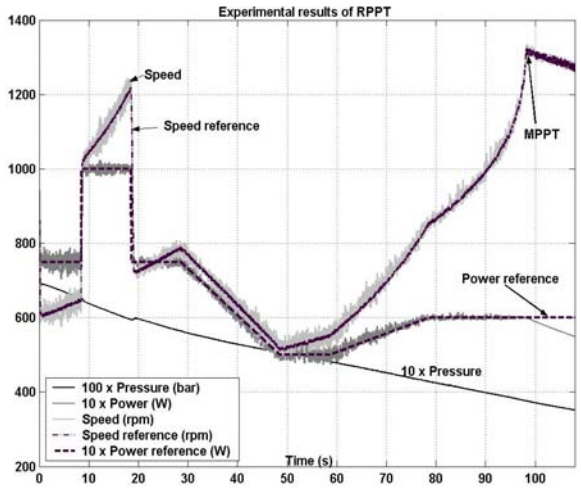


**Figure 12: Experimental results of RPPT Strategy.**

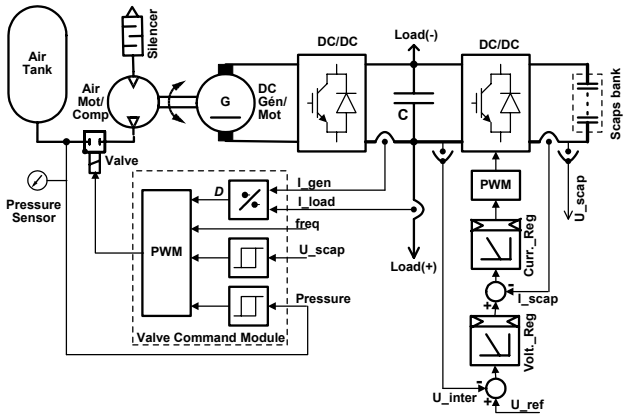


**Figure 13: Principle of output power variation**

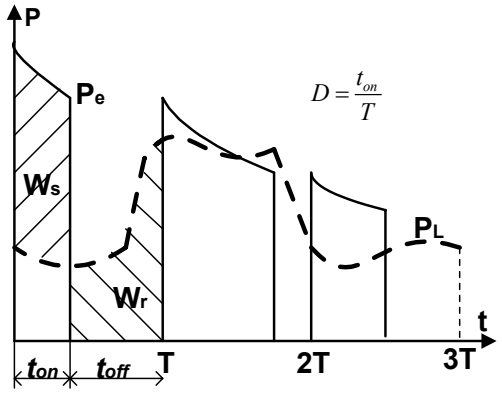


**Figure 14: Power modulation**

### 4.2- Fixed Frequency Operation Mode

In this mode, the on-off cycle period ***T*** of the thermodynamic conversion is constant. The converted energy $W_e$ is then proportional to the duty cycle ***D*** as shown in Figure 14. As the reservoir pressure drops during operation, the produced power $P_e$ decreases. When the system is suitably adjusted, the energy $W_s$ stored during the running time $t_{on}$ is equal to the energy $W_r$ required by the load during the stop time $t_{off}$ .

$$W_s = W_r \Leftrightarrow \int_0^{D.T} P_e dt = \int_0^{T} P_L dt \qquad (16)$$

If we consider the simple but improbable case where the produced power $P_e$ and the load power $P_L$ are constant, we can get from equation (16) the Duty cycle:

$$D = P_L / P_e \qquad (17)$$

Since it's not possible to predict the behavior of the load power, ***D*** is determined once at the beginning of each cycle using relation (17). This approach is accurate only if the cycle period ***T*** is small enough compared to the time constant of the powers. It may happen that the load power increases strongly within a cycle in such a way that the stored energy becomes insufficient to supply the load. In that case, the pneumatic machine is turned on as soon as the minimum allowable value of the supercapacitive bank voltage is reached. It's also turned off at the maximum supercapacitive bank voltage and the minimum operating pressure as can be seen on figure 13. The simulation results of this mode are presented in figure 15. As it can be seen, the cycle period is not always constant, particularly when the load power is important and the supercapacitive bank discharged.

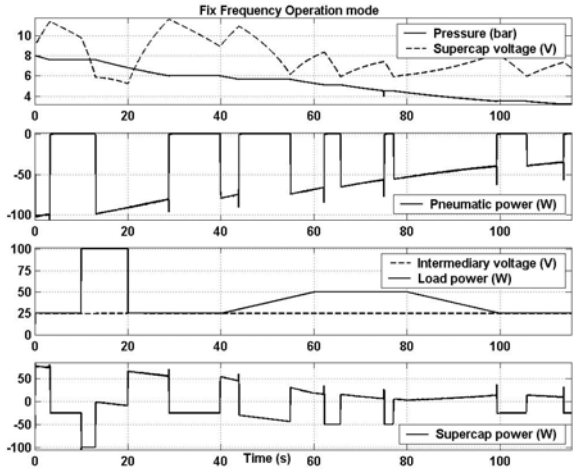


**Figure 15: Fix Frequency Operation mode**

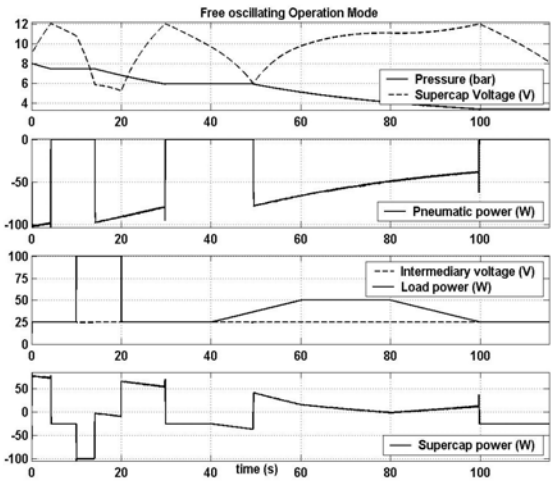


**Figure 16: Free oscillating Operation mode**

**4.3- Free oscillating Operation Mode**

In this mode, the operation cycle period is not constant. The only control parameter is the supercapacitive bank voltage. When it reaches the minimum value, the pneumatic motor is turned on and when it reaches the allowed maximum, the motor is turned off. As the intermediary voltage is held constant, the frequency and duty cycle of the operation cycle is automatically fitted to the ratio between $P_e$ and $P_L$. This is the simplest way to modulate the produced power. As it can be seen from the simulation results presented in figure 16, within the same generation conditions, the number of turn-on and offs of the pneumatic machine is lower than in the previous mode.

**4.4- Sizing the Supercapacitive bank**

The supercapacitive bank must be able to provide the energy $W_{Loff}$ required by the load during the time $t_{off}$ :

$$W_{Loff} = \int_{D.T}^{T} P_L dt \qquad (18)$$

The most critical case is where $D = 0$ and $P_L = P_{L\max} = C^{ste}$. In that case, we have:

$$W_{Loff\max} = T.P_{L\max} . \qquad (19)$$

The maximum amount of energy $W_{Sc\max}$ that can be stored in a supercapacitive bank of total capacitance $\boldsymbol{C_T}$ and maximum voltage $U_{T\max}$ is: $W_{Sc\max} = \frac{1}{2} C_T U_{T\max}^2$. But, because of the losses in the supercapacitors and the minimum voltage $U_{T\min}$ required by the interface converter, this energy cannot be restored totally. If we consider a discharge ratio ***d,*** ( $d = \frac{U_{T\min}}{U_{T\max}} \times 100\%$ ) and total discharge efficiency $\eta_d$, the maximum useful energy $W_{u\max}$ is: [12]

$$W_{u\max} = \frac{1}{2} \eta_d C_T U_{T\max}^2 \left[ 1 - \left( \frac{d}{100} \right)^2 \right] \qquad (20)$$

From equations (19) and (20) we can get $C_T$ as:

$$C_T = \frac{2T.P_{L\max}}{\eta_{cd} U_{T\max}^2 \left[ 1 - \left( \frac{d}{100} \right)^2 \right]} \qquad (22)$$

This design criterion takes into account that internal losses are produced inside the supercapacitive bank, because of the internal resistance. A more accurate design should also include the losses inside the interface converter.

**5- Conclusion and further works**

Compressed air in vessel storage systems have been considered so far as non-cost-effective, mainly because of the high price and volume of vessels along with cost and efficiency considerations on small turbo machinery [10]. But in the meantime, important technological improvements have been made on storage devices, namely with fiber-wound composites and stainless steel. The Efficiency optimization strategy proposed in this study can significantly improve the efficiency of the thermodynamic conversion. The presented topology, which combines compressed air and supercapacitors, improves the flexibility and dynamic performances of the storage system and makes it suitable for a wide range of low power autonomous and grid-connected applications, like renewable support and power quality enhancement for sensitive users. The typical advantages over classical CAES plants include site independence, fuel free operation and environmental harmlessness.

However, low pressure and low efficiency are weak spots of the studied system and are mainly related to the experimental pneumatic motor. The energy density of such vessel storage system can be improved by compressing air at higher pressures. This is possible today with the new light vessels mentioned above, which can handle pressure more than 300bar. To improve the efficiency of the thermodynamic conversion, the dedicated system should be able to operate at high and variable pressure in an isothermal process. For this

purpose, hydraulic machines offer the best performances, but they need a particular air-oil interface. Some of which have been proposed [13], but further developments are still required for such system to become reliable. Works are currently in progress in our institute to find power electronic solutions for flexible, efficient and reliable hydro-pneumatic storage systems.

**References**


[1] H. Stemmler, H. Voegele, G. Galasso; "Pump-Turbines with pole changing or variable speed motor generators", CICEM 1991

[2] L. Terens, R. Schäfer, " Variable speed in hydropower generation utilizing frequency converters," Water Power 93, proceedings of International Conference on Hydro Power, Nashville, Tennessee, 08/93.

[3] W. Seele, "Batteriespeiranlagen in elektrischen netzen," ABB – Technik, 1/89, pp 23-28

[4] A. Rufer, P. Barrade, "A Supercapacitor-Based Energy Storage System for Elevators with a Soft Commutated Interface," IEEE Trans. on Industry Applications, Vol. Sept October 2002.

[5] Bradshaw Ted D, "TVA Regenesis Vanadium Redox Flow" ESA Electricity Storage Association, Spring meeting, 2001, Chattanooga Te, April 2001.

[6] J. Siemer, "Stromversorgungsnetz heute und in Zukunft" Photon, das solarostrom Magazin, 7/2003, Solar Verlag GmbH 52070 Aachen.

[7] J. Lehmann, " Air storage gas turbine power plants, a major distribution for energy storage," International Conference on Energy storage, Brighton UK, April 29 – May 1 1981, pp 327 – 336.

[8] Van der Linden Septimus, "EESAT 02 Conference on Electrical Energy Applications and Technologies," San Francisco, April 2002

[9] C. Hua, C. Shem, "Comparative Study of Peak Power Tracking Techniques for Solar System" Proceedings of the IEEE.

[10] S. M. Schoenung, C. Burns; "Utility Energy Storage Applications Studies"; IEEE Transaction on Energy Conversion. Vol.11 N°3 September 1996.

[11] Kam W. Li; "Applied Thermodynamics: Availability Method and Energy Conversion"; Taylor & Francis, 1995

[12] P. Barrade, A. Rufer; "Energy storage and applications with supercapacitors"; ANAE, 23-26 March 2003, Bressanone, Italy

[13] A. Reller, I. Cyphelly; Speicherung gasförmiger energienträger – Eine Bestandsaufnahme, VDE – Berichte 1734, Energiespeicher, p.p. 37 – 45.

[14] R. Pandian, F. Takemura, Y. Hayakawa, S. Kawamura; "Control Performance of an Air Motor"; Proceedings of the 1999 IEEE Conference on Robotic & Automation.